

Instabilities and modes of collisionless stellar disks

C. Hunter¹

Department of Mathematics, Florida State University, Tallahassee, FL
32306-4510, U.S.A.

Abstract. Kalnajs's matrix method for calculating the normal modes of oscillation and instabilities of collisionless stellar disks has been used very sparingly since its publication 25 years ago. The fullest applications have been to singular scalefree disks for which the dynamics simplifies. This paper discusses some of the difficulties of implementing the method, and describes some ways of overcoming them. It also discusses circumstances in which true modes of oscillation, free from Landau damping, can exist.

1. Introduction

Kalnajs (1971,1977) formulated a matrix method for calculating the normal modes of oscillation and instabilities of collisionless stellar disks. Remarkably few successful applications of his method have been published since then. Kalnajs (1978) gave only limited results for an isochrone disk. The most successful applications have been to singular disks, first by Zang (1976) to scalefree isothermal disks, and more recently by Evans & Read (1998a,b) to scalefree disks with a range of different power-laws. Sawamura (1988) applied the method to a mildly non-uniformly rotating disk with a potential quadratic in r^2 , while Vauterin & Dejonghe (1996) studied a double Kuzmin-Toomre disk with a rotation curve that is close to flat outside a smooth core. Palmer & Papaloizou (1990) used the matrix to study $m = 1$ instabilities in the presence of counter-rotation, but simplified the orbits as epicycles. The matrix method is by no means restricted to the disk geometry and has been applied successfully to spherical systems, first in a pioneering study by Polyachenko & Shukman (1981), and subsequently by Palmer & Papaloizou (1987, 1988), Bertin et al (1989), Saha (1991) and Weinberg (1991a). These applications have focussed on the radial orbit instability.

2. The Matrix Method

The equilibrium state of a stellar disk is described by a distribution function f of stars moving on orbits in a circularly-symmetric potential $\Phi(r)$. The response of those orbits to a perturbed potential $\Phi'(r, \theta, t)$ can be calculated from the collisionless Boltzmann equation (Binney & Tremaine 1987). We search

¹Supported by National Science Foundation grants DMS-9704615 and DMS-0104751

for modes or instabilities with dependence on $e^{i(m\theta - \omega t)}$, where m is the angular wavenumber, and ω is the frequency. We represent the perturbed potential as

$$\Phi'(r, \theta, t) = e^{i(m\theta - \omega t)} \sum_j a_j \psi_j(r), \quad (1)$$

in terms of some set of potentials $\psi_j(r)e^{im\theta}$ whose mass densities $\sigma_j(r)e^{im\theta}$ are known and form a biorthonormal set. The response generates the density

$$\sum_j \sum_k M_{jk} a_k \sigma_j(r), \quad (2)$$

and self-consistency requires that

$$\sum_k M_{jk} a_k = a_j. \quad (3)$$

The components of the matrix M are the following integrals over the space of the actions J_r and J_θ :

$$M_{jk} = -(2\pi)^2 \iint dJ_r dJ_\theta \sum_{\ell=-\infty}^{\infty} \frac{[\ell \frac{\partial f}{\partial J_r} + m \frac{\partial f}{\partial J_\theta}] \widehat{\Psi}_{j,\ell} \widehat{\Psi}_{k,\ell}}{(\ell \Omega_r + m \Omega_\theta - \omega)}. \quad (4)$$

The denominator terms, which can cause the integrals to be singular, contain the two fundamental frequencies of oscillation in the two polar coordinates.

$$\Omega_r = \frac{\partial H}{\partial J_r}, \quad \Omega_\theta = \frac{\partial H}{\partial J_\theta}. \quad (5)$$

The numerator terms

$$\begin{aligned} \widehat{\Psi}_{k,\ell}(J_r, J_\theta) &= \frac{1}{\pi} \int_0^\pi \psi_k(r) \cos[\ell w_r + m(w_\theta - \theta)] dw_r, \\ &= \frac{1}{\pi} \int_{r_{\min}}^{r_{\max}} \psi_k(r) \cos[\ell w_r + m(w_\theta - \theta)] \frac{dr}{|\dot{r}|}, \end{aligned} \quad (6)$$

are Fourier coefficients of the potential functions which are obtained by integrating over an orbit. The angle variables w_r and w_θ describe the conditionally periodic motion on the orbital tori in phase space defined by the two actions. Many Fourier coefficients are needed. Although different angular wavenumbers m can be considered separately, Fourier coefficients are needed for each radial wavenumber ℓ , for each orbit, i.e. for each (J_r, J_θ) , and for each potential component ψ_k . The Fourier analysis is simpler when a disk is scalefree, because there is then only a one-parameter family of orbits.

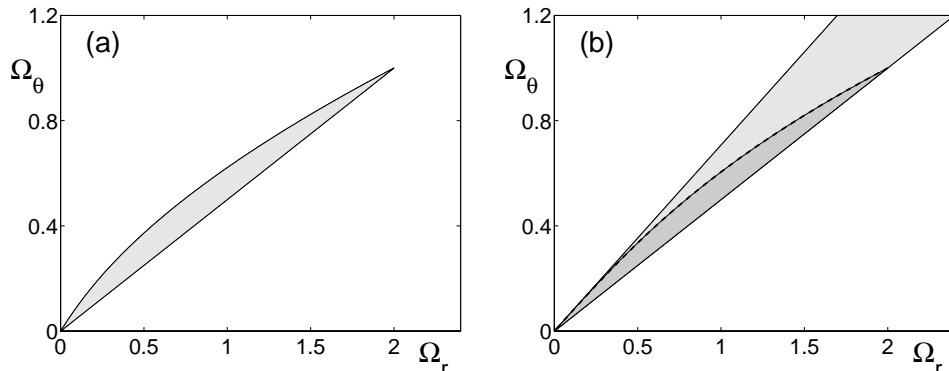


Figure 1. All directly-rotating bound orbits lie within the shaded regions of frequency space for (a) the Kuzmin-Toomre potential $\Phi(r) = -(1 + r^2)^{-1/2}$, and (b) the singular isothermal potential $\Phi(r) = \ln r$. Counter-rotating orbits occupy similarly shaped mirror-image regions below the Ω_r -axis. The more deeply shaded region in (b) is that for bound orbits in the cored isothermal potential $\Phi(r) = \ln(1 + r^2)/2$. The bound-orbit region is an angular sector for all scalefree potentials $\Phi(r) = r^\alpha/\alpha$ with $-1 \leq \alpha \leq 2$, is largest in the isothermal limit of $\alpha = 0$, and shrinks to a line in the two extreme cases of the Keplerian $\alpha = -1$ and harmonic $\alpha = 2$ potentials (Touma & Tremaine 1997).

3. Orbit populations

All orbits in the circularly-symmetric unperturbed potential $\Phi(r)$ have two isolating integrals of motion. These are commonly chosen to be the energy E and angular momentum L , but alternative choices are possible provided that they identify orbits uniquely. The alternative of the actions J_r and $J_\theta = L$ arises when action-angle variables are used in the derivation of the matrix equation (3). The turning radii r_{\max} and r_{\min} , which characterize the shape of the rosette orbits, can also be used (Hunter 1992, Vauterin & Dejonghe 1996). Another choice, which is relevant to the form of the matrix elements (4), is that of the orbital frequencies Ω_r and Ω_θ . Figure 1 shows the regions of the $(\Omega_r, \Omega_\theta)$ frequency space in which bound orbits lie. The form in Figure 1a is generic to potentials with a central core, while the outer form in Figure 1b is generic to scalefree potentials. In all cases, the upper boundary is formed by circular orbits for which Ω_r is the epicyclic frequency κ , and Ω_θ is the angular velocity Ω_c of circular motion. The lower boundary corresponds to radial orbits for which $\Omega_\theta = \Omega_r/2$. The slimness of the bound-orbit region is related to the fact that $\Omega_c - \kappa/2$ varies little over the whole range of a cored potential, as Lindblad (1959) noted for the Milky Way, and as Figure 6-10b of Binney & Tremaine (1987) for an isochrone potential shows. Figure 1a shows more generally that $\Omega_\theta - \Omega_r/2$ is small for orbits of *all* shapes, and not just for epicycles. This property has significant consequences in §4. The difference $\Omega_\theta - \Omega_r/2$ becomes large near the center for singular potentials in Figure 1b, as also in Figure 6-10a of Binney & Tremaine

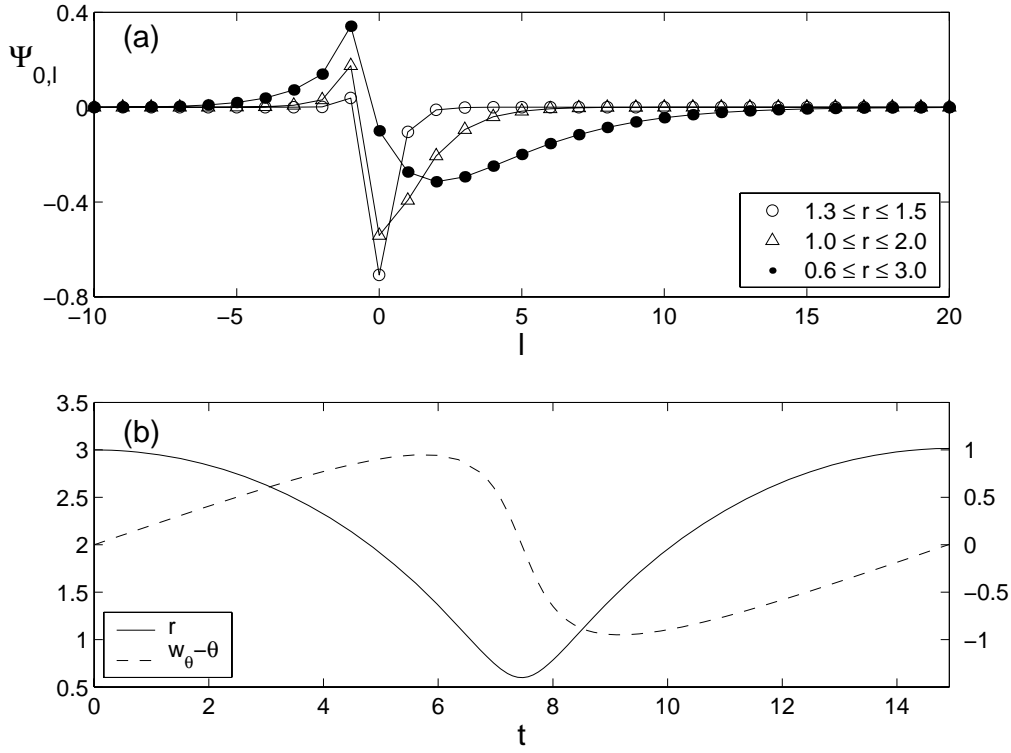


Figure 2. (a) Fourier coefficients $\hat{\Psi}_{0,\ell}(J_r, J_\theta)$ for the angular wavenumber $m = 2$, as functions of the index ℓ , for the orbits with the given ranges, and for the simplest potential $\psi_0(r)$ which has no sign changes. (b) The radial position and the lag of the angular position θ behind the angle variable w_θ for the widest ranging orbit of (a). The left hand scale is for r , and the right hand one for $w_\theta - \theta$.

(1987). Orbits near the center have the highest frequencies, while those at large distances lies at small frequencies.

4. Fourier analysis of orbits

There is a well-known theorem of Fourier analysis that the Fourier coefficients (6) for any orbit in any smooth potential ultimately decay exponentially rapidly with their index ℓ simply because motion in the radial variable r is periodic in the angle w_r . However the theorem says nothing about the rate of this decay, and it can be quite slow in ℓ . For a nearly circular orbit, r and $(w_\theta - \theta)$ both have small variations which are nearly sinusoidal in time. Such an orbit is well represented by three Fourier coefficients, a dominant one with $\ell = 0$, and two smaller ones with $\ell = \pm 1$. Figure 2a shows how the decay with increasing ℓ becomes markedly slower as the orbit becomes more eccentric. Figure 2b shows that the primary reason for this is the non-uniformity of the motion in $(w_\theta - \theta)$. Exponential decay in ℓ does not occur until ℓ is large enough for variations in

$\cos(\ell w_r)$ to be sufficiently rapid to cause cancellations in the regions of most rapid change. Hence, as Zang (1976) first found, many Fourier coefficients may be required for the accurate representation of an eccentric orbit. Much more extreme orbits than that of Figure 2b are included when distribution functions of the standard $f(E, L)$ form are used.

5. Resonances, and the accurate and efficient computation of the Matrix

An orbit is resonant with a wave with dependence on $e^{i(m\theta - \omega t)}$ if its frequency $\omega = \ell\Omega_r + m\Omega_\theta$ for some integer ℓ . A resonance causes the integrals which define the matrix elements (4) to be singular. These singular integrals must be evaluated according to Landau's (1946) rule; that is they must be obtained from analytical continuation of exponentially growing solutions with $\text{Im}(\omega) > 0$. Consequently the matrix elements (4) are generally complex-valued for a real resonant frequency ω because their defining integrals are sums of real principal value integrals and pure imaginary contributions from the residues at the resonance.

5.1. Computation of the Matrix M

Equation (3) shows that instabilities and modes are found by searching for frequencies ω for which the matrix M has a unit eigenvalue. This search is necessarily iterative because of the nonlinear dependence of M on ω , and hence requires repeated evaluations of M . Here we describe a method which simplifies those evaluations and which evaluates their singular integrals accurately. We integrate over the frequency space of Figure 1. We use the oblique coordinate $\xi = \ell\Omega_r + m\Omega_\theta$ as one integration variable, and some other independent coordinate η as the other. We integrate in η first. This gives an integral of the form $\int_{\xi_{\min}}^{\xi_{\max}} F(\xi) d\xi / (\xi - \omega)$. This integral is then converted to the standard form $\int_{-1}^1 F(\bar{\xi}) d\bar{\xi} / (\bar{\xi} - \bar{\omega})$, in the variables $\bar{\xi}$ and $\bar{\omega}$ which are obtained by the shifting and scaling transformations $\bar{\xi}(\ell) = 2(\xi - \xi_{\min}) / (\xi_{\max} - \xi_{\min}) - 1$ and $\bar{\omega}(\ell) = 2(\omega - \xi_{\min}) / (\xi_{\max} - \xi_{\min}) - 1$. (Note the ℓ -dependence of $\bar{\xi}$ and $\bar{\omega}$; the limits ξ_{\max} and ξ_{\min} vary widely with ℓ .) We expand the function $F(\bar{\xi}) = \sum_{n=0}^{\infty} \alpha_n P_n(\bar{\xi})$ in Legendre polynomials. Then Neumann's formula (Abramowitz & Stegun 1965, eq. [8.8.3]), gives the matrix elements as

$$M_{jk}(\omega) = \sum_{\ell=-\infty}^{\infty} \left\{ -2 \sum_{n=0}^{\infty} \alpha_n(j, k, \ell) Q_n[\bar{\omega}(\ell)] \right\}. \quad (7)$$

Here the Q_n are Legendre functions of the second kind. The expansion and integration over frequency space can all be done implicitly, and the coefficients α_n all evaluated by the following integrations over action space which are free of singularities:

$$\alpha_n(j, k, \ell) = \frac{-4(2n+1)\pi^2}{(\xi_{\max} - \xi_{\min})} \iint \left[\ell \frac{\partial f}{\partial J_r} + m \frac{\partial f}{\partial J_\theta} \right] \hat{\Psi}_{j,\ell} \hat{\Psi}_{k,\ell} P_n(\bar{\xi}) dJ_r dJ_\theta. \quad (8)$$

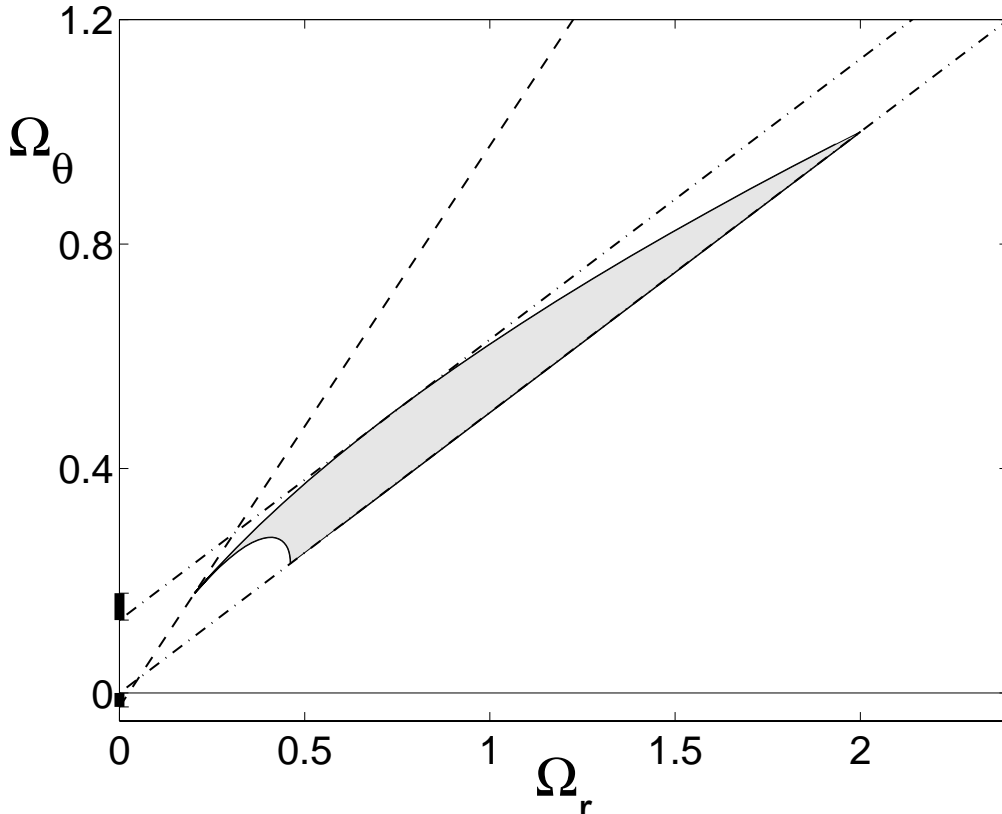


Figure 3. Frequency space for a Kuzmin-Toomre disk for orbits which are confined to the region $r \leq 3$. The dot-dashed lines have slope 0.5 and the dashed line has unit slope. As explained in the text, the thick sections of the Ω_θ -axis are gaps in which there can be discrete $m = 2$ modes.

Note the dependency of the α_n ; there is a different set for each orbit, for each n , and for each radial wavenumber ℓ . But once they have been obtained, the matrix elements can then be evaluated rapidly for any frequency from the double sum (7). The Legendre Q -functions have branch point singularities at $\bar{\omega} = \pm 1$. Landau's rule is satisfied by taking branch cuts from those singularities to be in the lower half $\text{Im}(\bar{\omega}) < 0$ of the complex $\bar{\omega}$ -plane.

5.2. Discrete modes

Mathur (1990) has shown how collisionless stellar systems can have true oscillatory modes which are free from Landau damping. Such modes occur in gaps in the continuous spectrum. Orbits for the one-dimensional systems and radial modes of spherical systems which he considered have a single frequency Ω with a finite range. The gaps lie between the intervals $[\Omega_{\min}, \Omega_{\max}]$, $[2\Omega_{\min}, 2\Omega_{\max}]$, $[3\Omega_{\min}, 3\Omega_{\max}]$, etc. There is always a principal gap of frequencies which are less in magnitude than Ω_{\min} , but there may not be any others. There are none

unless $2\Omega_{\min} > \Omega_{\max}$. Mathur proved the existence of a discrete mode in the principal gap for one specific case. Weinberg (1991b) studied a one-dimensional model for the vertical oscillations of the Galactic disk and found discrete modes in the principal and other gaps.

Gaps in the continuous spectrum can occur for disks, and Figure 3 shows how. It shows the part of frequency space of a Kuzmin-Toomre potential for orbits which are confined to lie within the outer radius $r = 3$. There is then a least radial frequency Ω_r , and a principal gap has opened up for $m = 0$ radial modes. There is also a least angular frequency Ω_θ . Gaps for modes of angular wavenumber m can be found by sliding the center of a pencil of lines of slope ℓ/m for all integers ℓ , both positive and negative, up and down the Ω_θ -axis, and locating positions of the center for which no lines of the pencil cross any part of the orbital-frequency space. Such points correspond to possible values of ω/m for discrete modes. Figure 3 shows two such gaps for discrete $m = 2$ modes. The upper gap is $0.178 > \omega/2 > 0.130$. Its lower limit comes from the $\ell = -1$ line which is tangent to the upper edge of frequency space, and its upper from the least Ω_r of the outermost circular orbit. The lower is the gap of $0 > \omega/2 > -0.025$ between the $\Omega_\theta = \Omega_r/2$ lower boundary of frequency space, and the $\ell = -2$ line of slope 1 through its lower left hand corner. The whole range $0.178 > \omega > -0.025$ provides a gap for discrete $m = 1$ modes. Athanassoula & Sellwood (1986), who truncated a Kuzmin-Toomre disk at the radius $r = 6$, for which the upper $m = 2$ gap of Figure 3 does not exist because the lower left hand corner of frequency space the lies at $(0.069, 0.067)$. They and Hunter (1992) found slow-growing instabilities with $\omega/2 > 0.130$, i.e. modes with no Lindblad resonances. But, as Weinberg (1991b, 1994) has noted, modes which are only weakly damped and which persist for long periods of time may occur either near the ends of gaps, or even when there are no gaps and only few resonant stellar orbits.

6. Summary

This paper has discussed ways of helping the Kalnajs Matrix method become a more effective tool for investigating instabilities and modes of collisionless stellar systems. These ways were developed when earlier investigations showed the need for them. They are now being incorporated in ongoing work. Orbital properties, as always, play a central role. It is surprising that the orbital frequencies Ω_r and Ω_θ have been so little used to characterize orbits. Orbital frequency space is helpful for clarifying the significance of resonances, and as a basis for our simplified and accurate method for evaluating matrix elements. With those simplifications, the Fourier analysis is the largest remaining computational task. Inordinately long Fourier series are needed for extremely eccentric orbits. Because there is no evidence that such orbits generally form a significant component of disk galaxies, it is simplest to select distribution functions which exclude them. There are several important issues which remain to be elucidated concerning instabilities and modes of disk galaxies. One which we have discussed is that of the existence and prevalence of long-lived modes. Another which we have scarcely mentioned is that of the stark differences which have been found between the behaviors of singular and cored models.

References

- Abramowitz M. & Stegun, I.A., 1965, Handbook of Mathematical Functions (New York: Dover)
- Athanassoula, E. & Sellwood, J.A. 1986, MNRAS, 221, 213
- Bertin, G., Pegaroro, F., Rubini, F. & Vesperini, E. 1994, ApJ, 434, 94
- Binney, J. & Tremaine, S. 1987, Galactic Dynamics (Princeton: Princeton Univ. Press)
- Evans, N.W., & Read, J.C.A. 1998a, MNRAS, 300, 83
- Evans, N.W., & Read, J.C.A. 1998b, MNRAS, 300, 106
- Hunter, C. 1992, Ann. N.Y. Acad. Sci., 675, 22
- Kalnajs, A.J. 1971, ApJ, 166, 275
- Kalnajs, A.J. 1977, ApJ, 212, 637
- Kalnajs, A.J. 1978, in IAU Symp. 77, Structure and Properties of Nearby Galaxies, ed. E.M. Berkhuisjen & R. Wielebinski (Dordrecht: Reidel) 113
- Landau, L.D. 1946, J. Phys. USSR, 10, 25
- Lindblad, B. 1959, in Handbuch der Physik, ed. S. Flügge (Springer: Berlin) 53, 21
- Mathur, S.D. 1990, MNRAS, 243, 329
- Palmer, P.L., & Papaloizou, J.P. 1987, MNRAS, 224, 1043
- Palmer, P.L., & Papaloizou, J.P. 1988, MNRAS, 231, 935
- Palmer, P.L., & Papaloizou, J.P. 1990, MNRAS, 243, 263
- Polyachenko, V.L. & Shukhman, I.G. 1981, Soviet Ast., 25, 533
- Saha, P. 1991, MNRAS, 248, 494
- Sawamura, M. 1988, PASJ, 40, 279
- Touma, J., & Tremaine, S. 1997, MNRAS, 292,90
- Vauterin, P. & Dejonghe, H. 1996, A&A, 313, 465
- Weinberg, M.D., 1991a, ApJ, 368, 66
- Weinberg, M.D., 1991b, ApJ, 373, 391
- Weinberg, M.D., 1994, ApJ, 421, 481
- Zang, T.A. 1976, The Stability of a Model Galaxy, Ph.D. dissertation, M.I.T.